Journal of Physics: Condensed Matter

ACCEPTED MANUSCRIPT

Half-auxetic effect and ferroelasticity in a two-dimensional monolayer TiSe

To cite this article before publication: Ziyuan Liu *et al* 2021 *J. Phys.: Condens. Matter* in press https://doi.org/10.1088/1361-648X/abdcea

Manuscript version: Accepted Manuscript

Accepted Manuscript is "the version of the article accepted for publication including all changes made as a result of the peer review process, and which may also include the addition to the article by IOP Publishing of a header, an article ID, a cover sheet and/or an 'Accepted Manuscript' watermark, but excluding any other editing, typesetting or other changes made by IOP Publishing and/or its licensors"

This Accepted Manuscript is **© 2020 IOP Publishing Ltd**.

During the embargo period (the 12 month period from the publication of the Version of Record of this article), the Accepted Manuscript is fully protected by copyright and cannot be reused or reposted elsewhere.
As the Version of Record of this article is going to be / has been published on a subscription basis, this Accepted Manuscript is available for reuse under a CC BY-NC-ND 3.0 licence after the 12 month embargo period.

After the embargo period, everyone is permitted to use copy and redistribute this article for non-commercial purposes only, provided that they adhere to all the terms of the licence https://creativecommons.org/licences/by-nc-nd/3.0

Although reasonable endeavours have been taken to obtain all necessary permissions from third parties to include their copyrighted content within this article, their full citation and copyright line may not be present in this Accepted Manuscript version. Before using any content from this article, please refer to the Version of Record on IOPscience once published for full citation and copyright details, as permissions will likely be required. All third party content is fully copyright protected, unless specifically stated otherwise in the figure caption in the Version of Record.

View the article online for updates and enhancements.

This content was downloaded from IP address 159.226.35.207 on 27/01/2021 at 03:18

IOP Publishing Journal Title
Journal **XX** (XXXX) XXXXXX https://doi.org/XXXX/XXXX

Half-auxetic effect and ferroelasticity in a two-dimensional monolayer TiSe

Ziyuan Liu [1], Jinbo Pan [1*], Yan-Fang Zhang[1] and Shixuan Du [1,2,3]

[1] Institute of Physics and University of Chinese Academy of Sciences, Chinese Academy of Sciences, Beijing 100190, China
[2] CAS Center for Excellence in Topological Quantum Computation, Beijing 100190, China
[3] Songshan Lake Materials Laboratory, Dongguan 523808, China

E-mail: jbpan@iphy.ac.cn

Received xxxxxx
Accepted for publication xxxxxx
Published xxxxxx

Abstract

Two-dimensional (2D) materials with both auxetic effect and ferroelasticity are rare, however, have great potential applications in next generation microelectromechanical and nanoelectronic devices. Here, we report the findings of an extraordinary combination half-auxetic effect and ferroelasticity in a single p2mm-type TiSe monolayer by performing first-principles calculations. The unique half-auxetic effect, namely the material expand laterally under both uniaxial tensile strain, and compressive strain, is reported and explained by considering both the nearest and the next-nearest interactions. The ferroelasticity is stemming from the degeneracy breaking of the *3d*-orbitals of Ti atoms in a distorted tetrahedron crystal field, or the so-called Jahn-Teller effect. The results provide a guideline for the future design of novel two-dimensional multiple functional materials at the nanoscale.

Keywords: monolayer TiSe, half-auxetic effect, ferroelasticity, two-dimensional materials

1. Introduction

Two-dimensional (2D) materials exhibit extraordinary physical properties which distinct from those in their three-dimensional counterparts due to the quantum confinement effect [1], and are regarded to have great application potentials in the next-generation electronic [2] [3] [4] [5], optoelectronic [6-7], electromagnetic devices [8]. Great efforts have been devoted to the investigation of 2D materials especially in the last decade, thousands of 2D materials were theoretically predicted, and their electronic properties were studied [9].

Despite the great success in the discovery and investigation of 2D functional electronic materials, the mechanical properties of 2D materials are less reported. Common materials undergo a transverse contraction (expansion) when they were stretched (compressed). However, the auxetic materials [10] undergo a transverse contraction (expansion) when compressed (stretched), and are promising candidates in biomedicine, fasteners [10], sensors, national security and defense[11-12], and other fields due to their largely increased mechanical toughness. The auxetic effect has been reported in a number of 2D materials, such as δ-phosphorene [13], monolayer BP_5 [14], 2D silicon dioxide [15], monolayer CaSi [16], 2D honeycomb structures [17] (graphene, silicene, *h*-BN, *h*-GaN, *h*-SiC and *h*-BAs). The origin of the auxetic effect in these 2D materials were attributed to pure geometric effect, pure electronic effect, or remain obscure in most of the cases.

Ferroelasticity represents the effect of the mechanical switching between at least two orientation states of a crystal by external stress [18] [19], and can be used to construct nonvolatile memory readable/writeable devices [20] at ambient conditions. The extraordinary combination of auxetic effect and ferroelasticity in a single compound makes the 2D material a highly versatile and promising in electromechanical at the nanoscale. However, because auxetic 2D materials and 2D ferroelastic materials are both rare, the discovery of 2D materials coexisting of these two intriguing properties is still limited to several exemplary materials [21] [22] [14] [23] [24].

In this study, using density functional theory based first principle calculations, we report that the monolayer TiSe[25-

Accepted Manuscript

 © xxxx IOP Publishing Ltd

26] in p2mm-type exhibits both half-auxetic effect[27] and ferroelasticity. Different from the traditional auxetic materials, which have a linear mechanical response to a uniaxial strain close to the equlibrium state, monolayer TiSe undergoes a transverse expansion no matter stretched or compressed under small strain, that is TiSe possesses a half-auxetic effect. This unusual mechanical behavior is elucidated by analyzing both the nearest neighboring Ti-Se interactions and also the next-nearest Ti-Ti interactions under strain. Under a suitable uniaxial tensile (compressive) strain along the short (long) axis direction, a ferroelastic switching occurs with a switching barrier of 0.25 eV. Since monolayer TiSe is dynamically and thermally stable, and its exfoliation energy is low (~0.025 eV/Å^2), it provides a promising platform for experimental investigation of the exotic properties and potential applications in nanoscale devices.

2. Methods

The structure and projected density of states calculations were performed by using the Vienna ab initio simulation package (VASP) code [28-29]. We used the density functional theory (DFT) within the generalized gradient approximation of the Perdew−Burke−Ernzerhof (PBE) functional [30]. A energy cutoff of 350 eV was used for the plane-wave basis set and 15×15×1 K-points was used to sample the Brillouin zone, 45×45×1 K-points was used when calculating the density of states. The vacuum length is 20 Å along the z axis. The monolayer TiSe was fully relaxed until the energy was converged to 10^{-8} eV and the maximum forces on each atom were below 0.001 eV/Å. A non-local correction function vdW-DF (optB86b-vdW) [31-32] was employed to consider the van der Waals interactions. Phonon spectrum was calculated using the DFPT method implemented in Phonopy code[33]. Ab initio molecular dynamics (AIMD) simulations were performed to estimate the thermal stability [34]. The solid-state nudged elastic band (SSNEB) method [35] was used to search the ferroelastic transition pathway.

To calculate the mechanical response of monolayer TiSe under uniaxial strain along *x*- (or *y*-) direction, the strain along *x*- (or *y*-) direction is fixed, and the strain along the other direction is allowed to relax until equilibrium. As a fundamental mechanical property, Poisson's ratio describes the negative ratio of transverse strain to infinitesimal longitudinal strain [36-37]. Similarly, we use the equations $-\frac{\varepsilon_y}{\varepsilon_x} = -\frac{a\Delta y}{b\Delta x}$ and $-\frac{\varepsilon_x}{\varepsilon_y} = -\frac{b\Delta x}{a\Delta y}$ to describe of magnitude of mechanical response to a large range of uniaxial strain along *x*- and *y*- directions, respectively. Here, *a* and *b* are the lattices constants of TiSe along *x*- and *y*- directions at equilibrium, Δx and Δy are the lattice constant deviations of TiSe along *x*- and *y*- directions under uniaxial strain, respectively.

3. Results and discussions

The layered bulk material of TiSe is obtained from the previous literature[38]. The optimized structure models of 2D TiSe monolayer with the space group p2mm are shown in figure 1(a). The primitive cell is labeled by a black rectangle, it contains two Ti atoms (grey) and two Se atoms (yellow). Each Ti atom is surrounded by four Se atoms. The relaxed lattice constants of monolayer TiSe are 4.40 Å and 3.57 Å along *x*-, and *y*- direction, respectively. Figure 1(b) presents a Brillouin zone marked by the high symmetry k-points. In order to estimate the dynamical stability of monolayer TiSe, we calculated the phonon dispersion as shown in figure 1(c). No imaginary frequency is observed, indicating that monolayer TiSe is dynamically stable. In addition, we also checked thermally stability of monolayer TiSe. The *ab initio* molecular dynamics (AIMD) simulation results in figure 1(d) clearly shows that after 5 ps there is neither structure reconstruction nor bond breaking at 300 K, implying the monolayer TiSe is thermally stable. To estimate the possibility of monolayer exfoliation from its bulk material, the normalized binding energies was calculated by $E_b = (E_{monolayer} - E_{bulk})/S$, where $E_{monolayer}$ and E_{bulk} are total energies of monolayer and bulk TiSe, and S is the area in the *xy*- plane. Van der Waals interaction was considered as described in the method part. The computed binding energy of TiSe is around 25 meV/Å^2, indicating the high possibility of monolayer exfoliation from the bulk material.

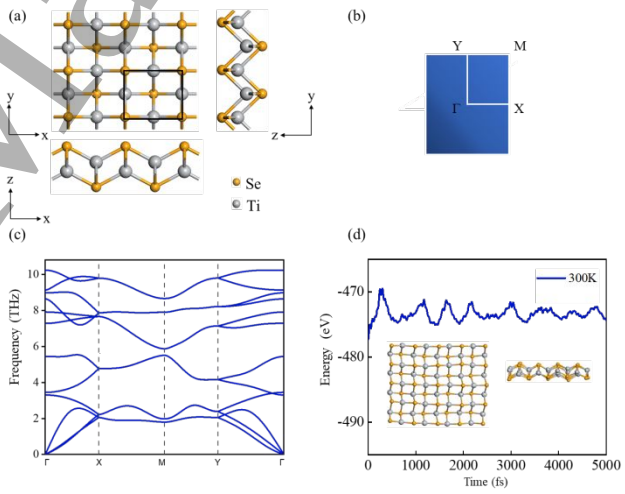

Figure 1. (a) Top and side views of monolayer TiSe, where grey atoms represent Ti atoms and yellow atoms represent Se atoms. (b) High-symmetry k-points in the first Brillouin zone of monolayer TiSe. (c) Phonon spectra of monolayer TiSe. (d) The ab initio MD simulations of monolayer TiSe at 300 K (after 5.0 ps).

Next, we proceed to examine the structural response to uniaxial strain and evaluate the resulting negative ratio of strain, as demonstrated in figure 2. The resultant lateral strain in response to a uniaxial strain in the range of ±7% applied

Accepted Manuscript

along the *x*- or *y*- direction is calculated. Non-linear variation of ε_y (or ε_x) to ε_x (or ε_y) can be observed. Under uniaxial strain along *x*- direction, a linear increasing of $-\frac{\varepsilon_y}{\varepsilon_x}$ as compressive strain is observed, while a non-linear variation of $-\frac{\varepsilon_y}{\varepsilon_x}$ as tensile strain is observed. Under uniaxial strain along *y*- direction, the mechanical response is different, indicating an anisotropy mechanical properties of TiSe. In this case, under compressive strain, the $-\frac{\varepsilon_x}{\varepsilon_y}$ firstly increases as strain and then reaches a platform. Under tensile strain, the curve decreases first, then linearly increases after it reaches a minimum value. A transition from negative to positive is observed at the tensile strain around 4%.

To understand this novel mechanical behavior under strain, a geometric structure evolution model is constructed as shown in figure 2(c). Here, we only qualitatively analyze the case that a uniaxial strain along *x*- direction is applied, since the mechanism of geometric evolution under a uniaxial strain along *y*- direction is similar. Under stretch, the Ti_1 atom moves to the left, while the Ti_2 atom moves to the right. The Se atom moves downward simultaneously due to the strong attractive interactions from Ti_1 and Ti_2 atoms. The downwards shift of Se atom further generates repulsive forces pointing from Se atom to Ti_3 and Ti_4 atoms. Meanwhile, the move of Ti_1 and Ti_2 atoms also induce the increasing of neighboring Ti-Ti distance. Figure 2(d) shows a bonding state below Fermi energy and an antibonding states above Fermi energy, which are contributed by d_{xy} orbitals of Ti atoms. This phenomenon indicates that the next-nearest interactions cannot be ignored. Overall, Ti_3 atoms undergo two forces, repulsive force F_{Se} from Se atom, and attractive force F_{12} from Ti_1 and Ti_2 atoms, as shown in the top-right panel in figure 2(c). If the included angle φ between resultant force and F_{12} is larger than 90º, an expansion of the lattice constant along *y*- direction occurs, auxetic effect of TiSe thus occurs. Inversely, if the included angle φ is less than 90º, no auxetic effect of the material occurs. Similarly, the geometric structure evolution under compression is shown in the bottom-right panel in figure 2(c). Ti_3 atoms undergo an attractive force from Se atom and a repulsive force from Ti_1 and Ti_2 atoms, the $-\frac{\varepsilon_y}{\varepsilon_x}$ is also determined by the direction of resultant force F_{tot}.

Under uniaxial strain along *x*- direction (or *y*- direction), both tensile strain and compressive strain lead to the expansion of TiSe in the *y*- direction (or *x*- direction) near the equilibrium state. This behavior is different from the typical 3D artificial auxetic materials in which the auxetic effect is totally a geometric effect, and also different from the recently reported 2D auxetic materials which have linear mechanical response to uniaxial strain, at lease under small longitudinally compression or stretch. This half-auxetic effect makes TiSe a good platform for the researches of novel functional applications.

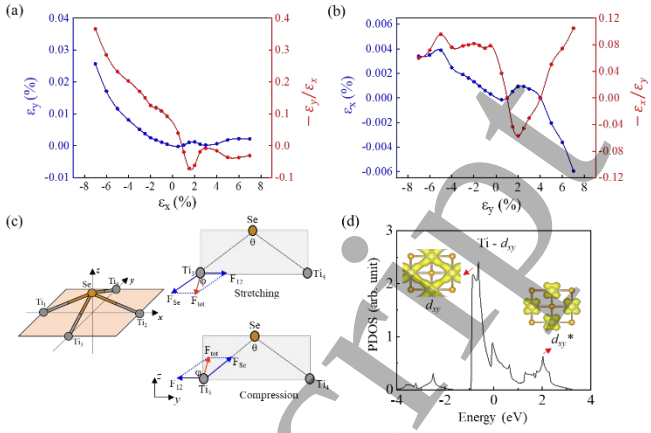

Figure 2. Mechanical response of monolayer TiSe under uniaxial strain along the (a) *x*- direction and (b) *y*- direction. (c) Geometric structure evolution model of monolayer TiSe under a uniaxial strain along *x*- direction. (d) Projected density of state (PDOS) and partial charge density of Ti-d_{xy} orbitals.

There are two stable orientation variants of monolayer TiSe named initial variant I and final variant III in figure 3(a). For the initial variant I, the larger lattice constant lies in the *x*-direction. After compressing (or stretching) it continuously along the *x*- (*y*-) direction, the larger lattice constant may switch to the *y*- direction, that is the final variant III, where |a′| = |b| and |b′| = |a|. From the analysis of the lattice constant, the final variant III can be obtained by rotating the initial variant I under 90° clockwise rotation. At the same time, during the compression process, there will be a square transition state with equal lattice constant in the *x*- and *y*- directions (|a| = |b|). The ferroelastic switching pathway between variant I and III was studied by using the solid-sate nudged elastic band (ss-NEB) method. As shown in figure 3(b), the intermediate variant connecting initial variant I and final variant III is the transition state II with a symmetry of p4mm, and its lattice constants along the *x*- and *y*- directions are equal, *a*=*b*. The energy barrier switching from initial variant I to transition state II is about 0.25 eV/atom, which is smaller than that of BP_5 (0.32 eV/atom) [14]. The overall geometric evolution of TiSe under tensile strain along *y*- direction contains several steps. Firstly, under small strain the lattice constant along *x*-direction increases due to large repulsive force from the top Se atom to the Ti atoms in the strain direction, resulting in an auxetic effect in TiSe. As further increasing the strain, the geometric structure then contracts along *y*- direction. From the transition state II to the initial state I and final state III, the geometric structure evolution processes are the same except that the directions are different. Relative to the initial state I of TiSe, the transition state II occurs at a stretch strain around 15% along y- direction.

Accepted Manuscript

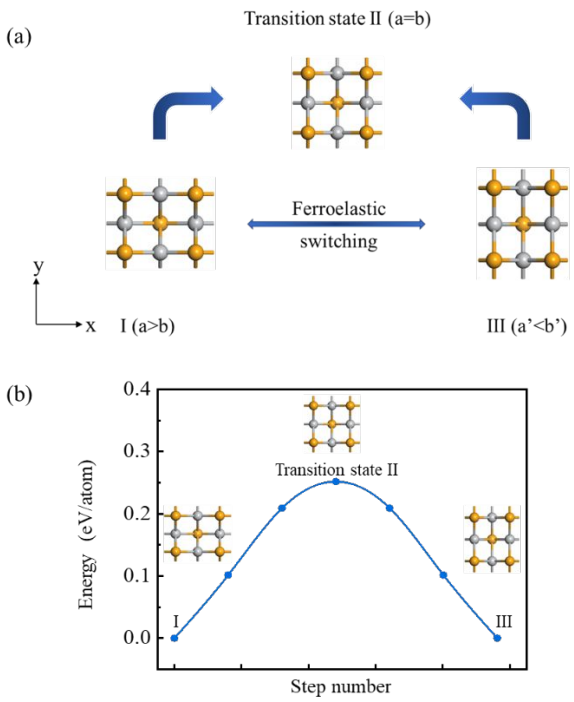

Figure 3. (a) Ferroelastic switching pathway of monolayer TiSe (I-II-III). (b) The energy profiles of ferroelastic switching as a function of step number in the solid-sate nudged elastic band (SSNEB) for monolayer TiSe.

Since the surrounding atoms of Se atom along *x*- and *y*-directions are the same, the origin of symmetry broken should come from the electronic structures. Figure 4 shows the projected density of states (PDOS) of monolayer TiSe on *3d*-ortibals of Ti atom under both ground state and transition state. At the transition state II, the TiSe has a p4mm plane group. The Ti atom and its four neighbouring Se atoms form a distorted tetrahedron. In this crystal field, the *3d*-orbitals splitting into four groups, $d_{xz}d_{yz}$, d_{xy}, d_{z^2}, $d_{x^2-y^2}$ as shown in figure 4(a). The d_{xz} and d_{yz} orbitals degenerate in this square lattice, as can be seen that the green and red curves are completely overlapped, and both orbitals are partially filled. When the structure is distorted from the square lattice to a rectangular lattice, the degenerated d_{xz} and d_{yz} orbitals split into two non-degenerated ones. Here in the variant I, the d_{xz} orbital goes down, while the d_{yz} orbital goes up. Our calculated results reveal that at the transition state II, both the d_{yz} and d_{xz} orbitals are occupied by 0.99 electrons. At the group state-variant I, these two orbitals are occupied by 1.22 and 0.81 electrons, respectively. This phenomenon is known as Jahn-Teller distortion, more electrons occupy the lower orbital and less electrons occupy higher orbital, thus lowers the total electronic energy, TiSe thus prefers the lattice with lower symmetry. Similar ferroelastic transition was theoretically predicted in α-SnO monolayer: from p2mm to p4mm, then to p2mm [39].

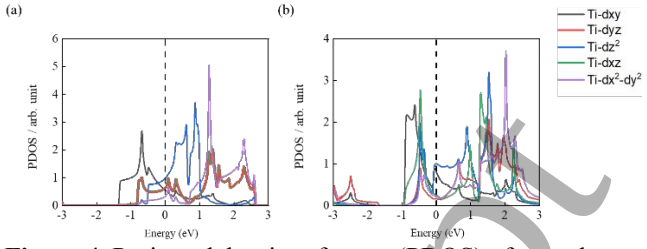

Figure 4. Projected density of states (PDOS) of monolayer TiSe (a) transition state II and (b) variant I.

4. Conclusions

In summary, by performing first-principles calculations, we predicted that p2mm-type TiSe monolayer is dynamically and thermally stable, and has a coexistence of a unique half-auxetic effect and ferroelastic property. The half-auxetic effect originates from the interplay of both the nearest and next-nearest interactions in a buckled geometric structure. Anisotropic mechanical properties along *x*- and *y*- directions are observed due to the geometric symmetry broken in these two directions. The ferroelastic switching can be achieved by applying tensile strain along short axis or compressive strain along long axis with a transition barrier of about 0.25 eV/atom. The origin of the ferroelasticity in TiSe is the Jahn-Teller effect, which breaks the degeneracy of partially occupied d_{xz} and d_{yz} orbitals of Ti atom, and lowers the energy. This exotic combination of half-auxetic effect and ferroelasticity make TiSe promising as multiple functional materials at the nanoscale.

Acknowledgements

This work was financially supported by National Nature Science Foundation of China (61888102), National Key Research and Development Projects of China (2016YFA0202300 and 2018YFA0305800), the Strategic Priority Research Program of the Chinese Academy of Sciences (XDB30000000). Computational resources were provided by the National Supercomputing Center in Tianjin.

ORCID iDs

Ziyuan Liu https://orcid.org/0000-0003-2203-612X

Jinbo Pan https://orcid.org/0000-0003-2612-8232

Yanfang Zhang https://orcid.org/0000-0002-9669-104X

Shixuan Du https://orcid.org/0000-0001-9323-1307

References

[1] Novoselov K S, Geim A K, Morozov S V, Jiang D, Katsnelson M I, Grigorieva I V, Dubonos S V and

Accepted Manuscript

Firsov A A 2005 Two-dimensional gas of massless Dirac fermions in graphene *Nature* **438** 197

[2] Li L K, Yu Y J, Ye G J, Ge Q Q, Ou X D, Wu H, Feng D L, Chen X H and Zhang Y B 2014 Black phosphorus field-effect transistors *Nat. Nanotechnol.* **9** 372

[3] Liu H, Neal A T, Zhu Z, Luo Z, Xu X F, Tomanek D and Ye P D 2014 Phosphorene: An Unexplored 2D Semiconductor with a High Hole Mobility *ACS Nano* **8** 4033

[4] Qiao J S, Kong X H, Hu Z X, Yang F and Ji W 2014 High-mobility transport anisotropy and linear dichroism in few-layer black phosphorus *Nat. Commun.* **5** 4475

[5] Xia F N, Wang H and Jia Y C 2014 Rediscovering black phosphorus as an anisotropic layered material for optoelectronics and electronics *Nat. Commun.* **5** 4458

[6] Wang Q H, Kalantar-Zadeh K, Kis A, Coleman J N and Strano M S 2012 Electronics and optoelectronics of two-dimensional transition metal dichalcogenides *Nat. Nanotechnol.* **7** 699

[7] Butler S Z, Hollen S M, Cao L Y, Cui Y, Gupta J A, Gutierrez H R, Heinz T F, Hong S S, Huang J X, Ismach A F, Johnston-Halperin E, Kuno M, Plashnitsa V V, Robinson R D, Ruoff R S, Salahuddin S, Shan J, Shi L, Spencer M G, Terrones M, Windl W and Goldberger J E 2013 Progress, Challenges, and Opportunities in Two-Dimensional Materials Beyond Graphene *ACS Nano* **7** 2898

[8] Gong C and Zhang X 2019 Two-dimensional magnetic crystals and emergent heterostructure devices *Science* **363** 706

[9] Haastrup S, Strange M, Pandey M, Deilmann T, Schmidt P S, Hinsche N F, Gjerding M N, Torelli D, Larsen P M, Riis-Jensen A C, Gath J, Jacobsen K W, Mortensen J J, Olsen T and Thygesen K S 2018 The Computational 2D Materials Database: high-throughput modeling and discovery of atomically thin crystals *2D Mater.* **5** 042002

[10] Lakes R 1987 Foam Structures with a Negative Poisson's Ratio *Science* **235** 1038

[11] Lipsett A W and Beltzer A I 1988 Reexamination of dynamic problems of elasticity for negative Poisson's ratio *J. Acoust. Soc. Am.* **84** 2179

[12] Woo S, Park H C and Son Y-W 2016 Poisson's ratio in layered two-dimensional crystals *Phys. Rev. B* **93** 075420

[13] Wang H, Li X, Li P and Yang J 2017 δ-Phosphorene: a two dimensional material with a highly negative Poisson's ratio *Nanoscale* **9** 850

[14] Wang H D, Li X X, Sun J Y, Liu Z and Yang J L 2017 BP_5 monolayer with multiferroicity and negative Poisson's ratio: a prediction by global optimization method *2D Mater.* **4** 045020

[15] Gao Z B, Dong X, Li N B and Ren J 2017 Novel Two-Dimensional Silicon Dioxide with in-Plane Negative Poisson's Ratio *Nano Lett.* **17** 772

[16] Wang Y, Qiao M, Li Y F and Chen Z F 2018 A two-dimensional CaSi monolayer with quasi-planar pentacoordinate silicon *Nanoscale Horiz.* **3** 327

[17] Qin G Z and Qin Z Z 2020 Negative Poisson's ratio in two-dimensional honeycomb structures *npj Comput. Mater.* **6** 51

[18] Aizu K 1970 Possible Species of Ferromagnetic, Ferroelectric, and Ferroelastic Crystals *Phys. Rev. B* **2** 754

[19] Salje E K H 2012 Ferroelastic Materials *Annu. Rev. Mater. Res.* **42** 265

[20] Dong S, Liu J M, Cheong S W and Ren Z F 2015 Multiferroic materials and magnetoelectric physics: symmetry, entanglement, excitation, and topology *Adv. Phys.* **64** 519

[21] Du Y C, Maassen J, Wu W R, Luo Z, Xu X F and Ye P D 2016 Auxetic Black Phosphorus: A 2D Material with Negative Poisson's Ratio *Nano Lett.* **16** 6701

[22] Kou L, Ma Y, Tang C, Sun Z, Du A and Chen C 2016 Auxetic and Ferroelastic Borophane: A Novel 2D Material with Negative Possion's Ratio and Switchable Dirac Transport Channels *Nano Lett.* **16** 7910

[23] Zhou L J, Zhuo Z W, Kou L Z, Du A J and Tretiak S 2017 Computational Dissection of Two-Dimensional Rectangular Titanium Mononitride TiN: Auxetics and Promises for Photocatalysis *Nano Lett.* **17** 4466

[24] Yuan J H, Mao G Q, Xue K H, Wang J F and Miao X S 2020 A new family of two-dimensional ferroelastic semiconductors with negative Poisson's ratios *Nanoscale* **12** 14150

[25] Wu Z J, Wang M Y and Su Z M 2007 Electronic structures and chemical bonding in diatomic ScX to ZnX (X = S, Se, Te) *J Comput Chem* **28** 703

[26] Sorensen J J, Persinger T D, Sevy A, Franchina J A, Johnson E L and Morse M D 2016 Bond dissociation energies of diatomic transition metal selenides: TiSe, ZrSe, HfSe, VSe, NbSe, and TaSe *J. Chem. Phys.* **145** 214308

[27] Lim T C 2019 Composite microstructures with Poisson's ratio sign switching upon stress reversal *Compos. Struct.* **209** 34

[28] Kresse G and Furthmuller J 1996 Efficient iterative schemes for ab initio total-energy calculations using a plane-wave basis set *Phys. Rev. B* **54** 11169

[29] Kresse G and Furthmuller J 1996 Efficiency of ab-initio total energy calculations for metals and

Accepted Manuscript

semiconductors using a plane-wave basis set *Comput. Mater. Sci.* **6** 15

[30] Perdew J P, Burke K and Ernzerhof M 1996 Generalized Gradient Approximation Made Simple *Phys. Rev. Lett* **77** 3865

[31] Klimes J, Bowler D R and Michaelides A 2010 Chemical accuracy for the van der Waals density functional *J. Phys.: Condens. Matter* **22** 022201

[32] Klimes J, Bowler D R and Michaelides A 2011 Van der Waals density functionals applied to solids *Phys. Rev. B* **83** 195131

[33] Togo A, Oba F and Tanaka I 2008 First-principles calculations of the ferroelastic transition between rutile-type and CaCl2-type SiO2 at high pressures *Phys. Rev. B* **78** 134106

[34] Barnett R N and Landman U 1993 Born-Oppenheimer molecular-dynamics simulations of finite systems: Structure and dynamics of $(H_2O)_2$ *Phys. Rev. B* **48** 2081

[35] Sheppard D, Xiao P H, Chemelewski W, Johnson D D and and Henkelman G 2012 A generalized solid-state nudged elastic band method *J. Chem. Phys.* **136** 074103

[36] Mott P H and Roland C M 2013 Limits to Poisson's ratio in isotropic materials-general result for arbitrary deformation *Phys. Scr.* **87** 055404

[37] Rouxel T 2007 Elastic properties and short-to medium-range order in glasses *J. Am. Ceram. Soc.* **90** 3019

[38] Ding Y, Wang Y L and Ni J 2009 Electronic and magnetic properties of 3d transition-metal selenides from first principles *Solid State Commun.* **149** 505

[39] Seixas L, Rodin A S, Carvalho A and Neto A H C 2016 Multiferroic Two-Dimensional Materials *Phys. Rev. Lett.* **116** 206803

Accepted Manuscript